Astron. Astrophys. 339, L49–L52 (1998)

ASTRONOMY AND ASTROPHYSICS

LETTER

Letter to the Editor

A molecular jet from SVS 13B near HH 7–11

R. Bachiller[1], **S. Guilloteau**[2], **F. Gueth**[3], **M. Tafalla**[1], **A. Dutrey**[2], **C. Codella**[1], **and A. Castets**[4]

[1] IGN Observatorio Astronómico Nacional, Apartado 1143, E-28800 Alcalá de Henares, Spain
[2] Institut de Radio Astronomie Millimétrique, 300 rue de la Piscine, F-38406 Saint Martin d'Hères, France
[3] Max-Planck-Institut für Radioastronomie, Auf dem Hügel 69, D-53121 Bonn, Germany
[4] Laboratoire d'Astrophysique, Observatoire de Grenoble, BP53, F-38041 Grenoble Cedex 9, France

Received 2 September 1998 / Accepted 5 October 1998

Abstract. We present interferometric images of the λ 1.3 and 3.5 mm continuum and the SiO J $= 2 \rightarrow 1$ emission towards the SVS 13/HH 7–11 vicinity. The continuum data resolve SVS 13 into two components separated by 14.″5 ($\sim$ 4300 AU) and having very similar millimeter properties: each of them has about 1 $M_\odot$ of circumstellar material and its emission is characterized by a spectral index of $\sim$ 2.5. One of the components, SVS 13B, lacks optical, near infrared, or cm-wave counterpart, and is only detectable at millimeter waves, a fact that suggests it represents an extremely embedded, Class 0 object. This source, in addition, powers a remarkably collimated molecular outflow as seen by a high velocity SiO jet. HH 12, HH 16, and HH 352 lie along the line of this jet, suggesting they are also excited by SVS 13B. Our observations highlight the star-formation richness of the HH 7–11 region which contains in a small area some of the youngest and most extraordinary outflows known.

Key words: stars: formation – interstellar medium: individual objects: SVS13B, HH7-11, NGC1333 – interstellar medium: jets and outflows – interstellar medium: molecules – radio lines: molecular: interstellar

1. Introduction

Class 0 sources, characterized by strong millimeter and submillimeter emission, represent the youngest known low-mass protostars (André et al. 1993). They power bipolar outflows with extreme properties, including high collimation, high velocity gas, and evidence for strong shocks (Bachiller 1996). Their young age ($\sim 10^4$ years) makes them rare (a list of 30 objects was compiled by Bachiller 1996), so each of them provides a precious oportunity to study the earliest stages of stellar birth. In this letter we present a high resolution study of the vicinity of HH 7–11, where we have identified a spectacular outflow powered by an extremely embedded Class 0 source.

The HH 7–11 chain lies 6′ south from NGC1333 (see optical image by Bally et al. 1996 for an overall view). It is associated with a bipolar outflow excited by SVS 13 (Strom et al. 1976) and detected in CO emission up to extremely high velocities (> 100 km s^{-1}, see Bachiller & Cernicharo 1990). Optical and infrared images (Bally et al. 1996, Hodapp & Ladd 1995) show that the vicinity of HH 7–11 is an exceptionally rich and complex site of star formation, with multiple and sometimes overlapping signpost of recent stellar birth. We have carried out deep interferometric observations of the HH 7–11 vicinity, and this letter discusses our first results. A discusion of CO 2$\rightarrow$1 data will be presented in a forthcoming paper.

Send offprint requests to: R. Bachiller

2. Observations

The observations were carried out in March 1998 with the IRAM 5-antenna interferometer at Plateau de Bure. Three configurations were used with baselines extending up to 176 m. The antennas were equipped with dual-channel SIS receivers. The 1.3 mm receivers were tuned at the CO J $= 2 \rightarrow 1$ frequency (230.538 GHz), whereas the 3 mm receivers were tuned simultaneously to SiO J $= 2 \rightarrow 1$ and $H^{13}CO^+$ J $= 1 \rightarrow 0$ (86.847 and 86.754 GHz, respectively). Typical SSB system temperature was 130 K at λ 3.5 mm and 300 K at λ 1.3 mm. The correlator was configured with a bandwidth of 20 MHz centered at the SiO J $= 2 \rightarrow 1$ frequency, and the data were smoothed to provide a resolution of 1 km s^{-1}. Some correlator units free of line emission were combined to measure the continuum in a band of 320 MHz at λ 1.3 mm, and 100 MHz at 3.5 mm. Phase and amplitude calibration was achieved by observing 3C84, which is close in the sky to HH 7–11. The flux density of 3C84 was 2.6 Jy at 230.5 GHz, and 4.7 Jy at 86.6 GHz. The typical rms phase noise on the longest baselines was 30° and 10° at λ 1.3 and 3.5 mm, respectively. A mosaic of 10 overlapping fields was observed in order to cover the central region of the HH 7–11 outflow. Images were produced using natural weighting and cleaned with the mosaic routines of the GILDAS package. The clean beam is 1.9$\times$1.2″(P.A. 50°) and 4.1$\times$3.0″(P.A. 54°) at λ 1.3 mm and 3.5 mm, respectively.

3. Continuum emission

Fig. 1 presents λ 1.3 and 3.5 mm continuum maps of the SVS 13 vicinity. These maps reveal the structure of the continuum mm-

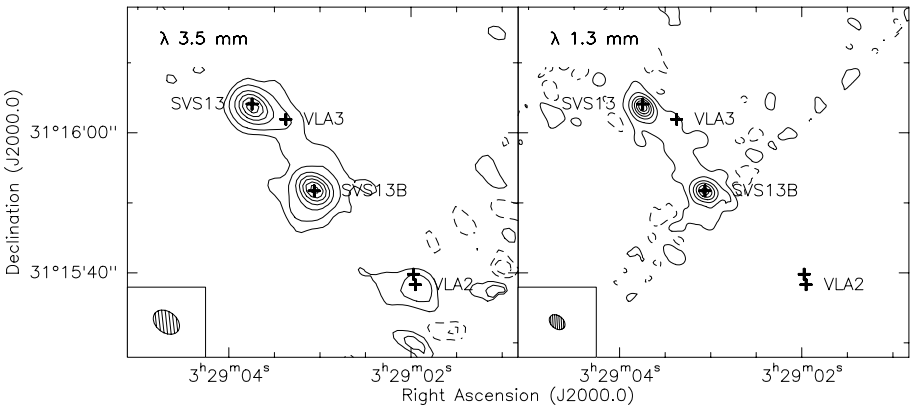

Fig. 1. Continumm mm-wave emission around HH 7–11. Contours are -2, -1, 1, 2, 4, 6,... mJy beam^{-1} (λ 3.5 mm map), and -40, -10, 10, 40, 80, 120,... mJy beam^{-1} (λ 1.3 mm map). The crosses mark the positions of the VLA sources reported by Rodríguez et al. (1997), and that of SVS 13B (this work). The clean beams are also indicated. The increase of noise at the map edges is due to the correction applied to account for the primary beam attenuation.

Table 1. Millimeter continuum sources in the HH 7–11 region.

Source name(s)			Position		Flux (mJy)		FWHM size at λ 1.3 mm		
			α (J2000)	δ (J2000)	λ3.5 mm	λ1.3 mm	Maj.($''$)	Min.($''$)	P.A.($^\circ$)
SVS 13	MMS 1	VLA 4	03:29:03.75	+31:16:03.7	26±1	320±10	1.53±0.09	1.01±0.08	16±7
SVS 13 B	MMS 2		03:29:03.06	+31:15:51.6	28±1	310±30	1.23±0.15		–
	MMS 3	VLA 2	03:29:01.92	+31:15:38.0	7±2				

Notes on SVS 13 and SVS 13B.- Positions, fluxes, and sizes were derived from fits in the *uv* plane, at 1.3 mm, of elliptical gaussian sources. Positions are accurate to within 0.″2. Fluxes are corrected for the primary beam attenuation. The reported 3.5 mm fluxes correspond to the gaussians derived from the 1.3 mm data. MMS sources refer to sources from Chini et al. (1997).

wave emission, which has been mapped with lower angular resolution by Chini et al. (1997) and Lefloch et al. (1998a). At both wavelengths, the maps are dominated by two strong peaks connected by a bridge of weak emission. There is a weaker third peak at the SW edge of the 3.5 mm map which unfortunately lies outside the interferometer field of view at 1.3 mm. The properties of the three compact sources, as well as the correspondence among designations used by different authors, are summarized in Table 1.

The strong source to the NE corresponds, within the positional uncertainties (0.″2), to the positions of SVS 13 and of the cm-wave source VLA 4, as determined by Rodríguez et al. (1997) with accuracies of 0.″3 and 0.″1, respectively. The source is somewhat elongated at 1.3 mm along P.A. 16±7°, i.e, approximately perpendicular to the HH 7–11 chain. Its size, at the assumed distance of 300 pc, is ∼450×300 AU.

The source to the SW coincides with the water maser spot H_2O(B) reported by Haschick et al. (1980), and with the position of VLA 2 of Rodríguez et al. (1997). This source, weak in the mm range, is the strongest source at cm wavelengths (Haschick et al. 1980, Rodríguez & Cantó 1983, Snell & Bally 1986).

Finally, the strong source at the map center coincides, within the observational uncertainties, with the position of the SVS 13B source detected by Grossman et al. (1987) at λ 2.7 and 3.1 mm. Our observations thus confirm the reality of this source, despite the doubts casted by Woody et al. (1989) and Sandell et al. (1990). The source is resolved and roughly circular: its size (after deconvolution of the beam) is 370±45 AU

As the continuum maps show, SVS 13 and SVS 13B are almost indistinguishable from their mm emission: they are very similar both in flux and size. This emission is not due to free-free radiation, since an extrapolation of the cm-wave fluxes from Rodriguez et al. (1997) leads to a negligible free-free contribution in the 1 to 3 mm range (< 6%). From our measurements at λ 3.5 and 1.3 mm we derive a spectral index α∼2.5 in both sources, but we caution that possible interferometer filtering of extended emission could result in an underestimate of the index. The value of α indicates that the emission arises from optically thin dust radiation, and if the dust mass opacity follows a power law of the form $\kappa_\nu \propto \nu^\beta$, then β∼0.5. This value is slightly smaller than the canonical $\beta = 1$, but agrees with values found in highly embedded objects (e.g. Ossenkopf & Henning 1995), which have been attributed to large (mm size) dust grains (Pollack et al. 1994).

Since the continuum represents thin dust emission, the total mass (gas and dust) of the circumstellar envelopes around SVS 13 and SVS 13B can be estimated from the mm fluxes. The major source of uncertainty in this estimate is the value of κ_ν, which depends upon the composition and shape of the dust grains. Pollack et al. (1994) suggest that at 1 mm, a value $\kappa_\nu \approx 0.005$ cm^2 g^{-1} encloses within a factor of 4 all the above uncertainties. Using such a value and assuming a dust temperature $T_{\rm d} \sim 20$ K, we obtain masses of $\sim 1\, M_\odot$ for both SVS 13 and SVS 13B.

Despite their similarities in the mm range, SVS 13 and SVS 13B are totally different at optical and infrared wavelengths. SVS 13 is a strong source in the infrared (Strom et al. 1976), and was even optically visible during an outburst (Mauron & Thouvenot 1991). SVS 13B, on the other hand, has neither optical nor near infrared counterpart, as can be seen in

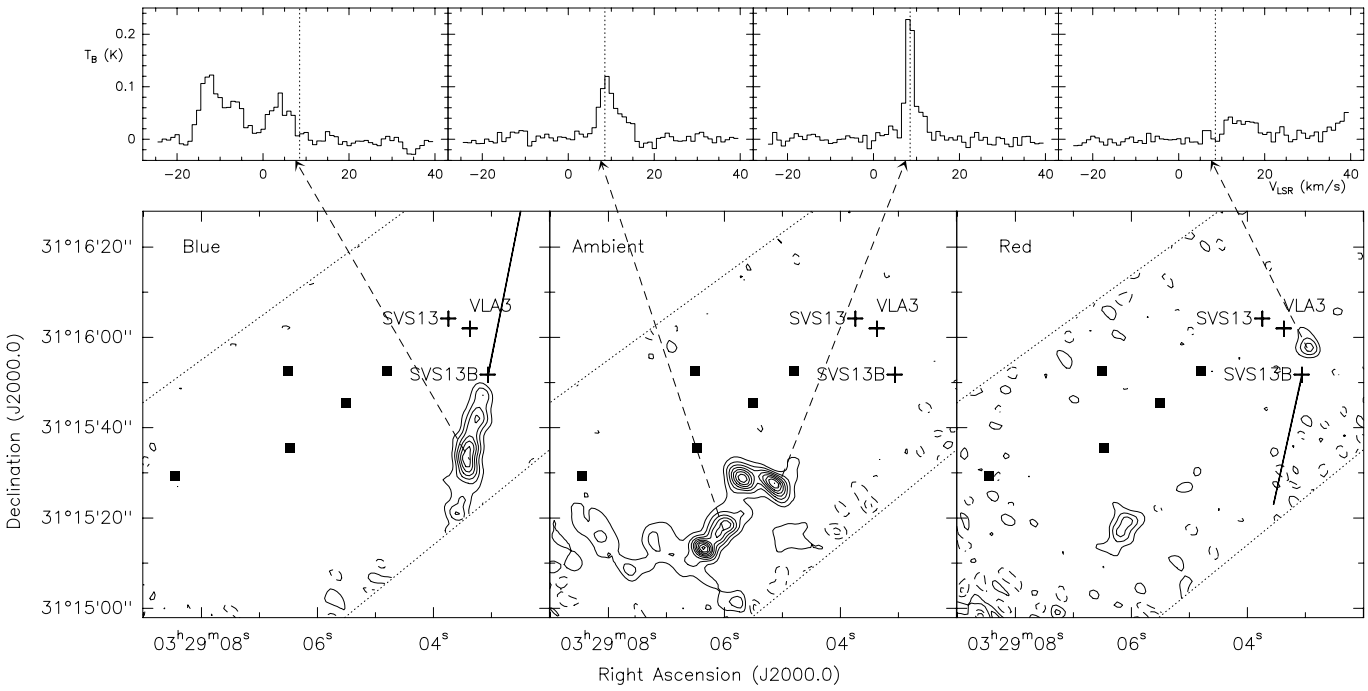

Fig. 2. Channel maps of the SiO J $= 2 \rightarrow 1$ line emission averaged over velocity intervals from -17 to 6.5 km s^{-1} (*left panel*), from 6.5 to 10.5 km s^{-1} (center), and from 10.5 to 17 km s^{-1} (*right*). First contour and step are 10 mJy beam^{-1}. The positions of the HH 7–11 objects are marked by black squares. Some spectra obtained at particular map positions are shown in the upper panels. The direction of the SiO jet driven by SVS 13B is indicated by the thick lines in the high velocity maps.

the sensitive images of Aspin et al. (1994) and Hodapp & Ladd (1995). This implies that SVS 13B is much more obscured than SVS 13. The luminosity of SVS 13 is 85 $L_\odot$(based on Molinari et al. 1993), while the luminosity of SVS13B can only be approximately estimated using mm obervations. Assuming that the spectral energy distribution of SVS 13B is similar to those of other deeply embedded sources, we estimate that this source has a total luminosity of $\sim 5\ L_\odot$.

Its unusually high mm-wave flux together with the lack of optical and infrared brightness strongly suggests that SVS 13B is a Class 0 source in the sense of André et al. (1993). This suggestion is strengthen by the unusual properties of SVS 13B's outflow, which we now turn to discuss.

4. A jet from SVS13 B

Fig. 2 shows SiO maps of the HH 7–11 vicinity for three velocity ranges. At ambient velocities (middle panel), there is a ridge of emission which coincides with the component seen at low resolution extending over the whole NGC1333 complex (Lefloch et al. 1998b, Codella et al. 1998). Comparing our SiO map with the CO maps of the HH 7–11 outflow by Bachiller & Cernicharo (1990), it seems that the low-velocity SiO emission delineates the compressed walls of the cavity opened by the extremely high velocity CO outflow from HH 7–11. This suggests that the narrow, low velocity SiO lines trace a shock-compressed shell within the ambient molecular cloud.

At blue velocities (left panel), the SiO emission appears elongated S-SE with PA 160°. It extends all the way down to the edge of the interferometer field of view, and continues for a total distance of $\sim 3'$, as indicated by the low resolution SiO maps of Lefloch et al. (1998b). SVS 13B lies very close to the tip of this emission, which arises from broad components in the spectra with velocities up to -20 km s^{-1}. Single dish data from Codella et al. (1998) show similar broad lines in SiO J $= 2 \rightarrow 1$, J $= 3 \rightarrow 2$, and J $= 5 \rightarrow 4$, implying the emission traces high excitation material. The red gas (right panel), on the other hand, forms two peaks, one to the south, with low velocity and probably associated with the extended ambient component, and the other faster and slightly north of SVS 13B. This second peak lies symmetrically opposed to the blue SiO filament, with SVS 13B as the center of symmetry, and reaches velocities up to $V_{LSR} > 40$ km s^{-1} (see feature in the spectra of Fig. 2, which extends outside our interferometer bandwidth). The maps in Fig. 2, therefore, show that the SiO emission has a bipolar distribution with respect to SVS 13B, with the red gas to the north and the blue gas to the south. This is strong evidence for a highly collimated molecular outflow powered by SVS 13B.

Further evidence for an outflow from SVS 13B comes from a comparison with 2.12 μm images, which trace shock excited H_2 and represent an independent outflow tracer. Hoddap & Ladd (1995) have imaged the HH 7–11 vicinity at this wavelength and identified a large number of H_2 features, not all of them associated with known flows. Their features 4 and 5, in particular, form a very narrow filament emerging from the vicinity of SVS13 and perfectly aligned with our blue SiO emission. Although Hoddap & Ladd (1995) (see also Lefloch et al. 1998a) suggest that this H_2 emission does not arise from an independent

outflow but from the interface between the SVS13 flow and the ambient cloud, our SiO data convincingly show this is not the case, and that the H_2 emission arises from the SVS 13B flow. The infrared images, in fact, show that the SVS 13B blue lobe forms one of the best collimated jets known, extending for more than $3'$ (~ 0.3 pc) without appreciable loss of collimation.

Unfortunately, the northern region of SVS 13B is not covered by the image of Hoddap & Ladd (1995), so we ignore whether a similar jet is present in the red side. Interestingly enough, $5'$ north of SVS13B lies one of the brightest HH objects in the sky, HH 12, whose exciting source still remains unidentified. The SiO jet from SVS 13B seems to point towards this HH object and the reversed proper motion vectors of HH 12 point back to the millimeter source (Herbig & Jones 1983). All this suggests that SVS 13B is the exciting source of HH 12, an idea previously advanced by Bally et al. (1996). We caution however that HH 12 is slightly blue shifted while the SiO jet is red, although this could be explained as resulting from velocity mixing due to the small inclination of the jet with the plane of the sky ($\sim$14° according to the HH 12 motion, see Herbig & Jones 1983). It is also interesting to note that a continuation of our SiO blue jet goes through the weak HH objects HH 16 and HH 352, $7'$ and $16'$ south of SVS 13B (Bally et al. 1996). HH 16 is in fact elongated along the line to SVS 13B, reinforcing a physical connection. If the SVS 13B outflow extends from HH 12 to HH 16, its total length is about $12'$, or $\sim$1 pc, and it could be as large as $\sim$2 pc if HH 352 is included.

Both the SiO and H_2 images show that the SVS 13B jet is very clumpy and consists of bright peaks connected by weaker emission, a common feature in molecular jets (e.g. Bachiller et al. 1991, Gueth et al. 1998). This is probably due to multiple shocks along the jet which alter the excitation and the molecular composition. The SiO abundance, in particular, most likely changes by orders of magnitude due to shock chemistry (e.g. Schilke et al. 1997, Caselli et al. 1997), and this makes it impossible to use this tracer to estimate the outflow mass and energetics. Further CO observations are therefore needed to fully characterize the energy properties of this unusual flow.

A parameter we can estimate from the SiO data is the kinematical timescale τ of the different knots. Asuming a space velocity of 100 km s^{-1} (i.e.: 25 km s^{-1} as measured from SiO – see Fig. 2 – deprojected for 14° inclination), the spacing between successive SiO knots corresponds to $\sim$ 200 yr, and the SiO knots closest to SVS 13B have $\tau < 100$ yr. The distant clumps seen in H_2 have $\tau \sim 4000$ yr, and the most distant HH objects would have $\tau \sim 13.000$ yr. These values confirm the extreme youth of the SVS 13B outflow, which together with its high collimation and extremely embedded exciting source are typical signatures of an outflow powered by a Class 0 protostar.

Acknowledgements. We are grateful to the IRAM staff for help with the observations, and to an anonymous referee for comments which led to improving the manuscript. RB acknowledges the hospitality from the Observatoire de Grenoble (France) and support from Spanish DGES grant PB96-104.

References

André P., Ward-Thompson D., Barsony M., 1993, ApJ 406, 122
Aspin C., Sandell G., Russel A.P.G., 1994, A&AS 106, 165
Bachiller R., 1996, ARA&A 34, 111
Bachiller R., Cernicharo J., 1990, A&A 239, 276
Bachiller R., Martín-Pintado J., Fuente A., 1991, A&A 243, L21
Bally J., Devine D., Reipurth B., 1996, ApJ 473, L49
Caselli P., Hartquist T.W., Havnes O., 1997, A&A 322, 296
Chini R., Reipurth B., Sievers A., et al. 1997, A&A 325, 542
Codella C., Bachiller R., Reipurth B., 1998, A&A , in press
Gueth F., Guilloteau S., Bachiller R. 1998, A&A 333, 297
Grossman E.N., Masson C.R., Sargent A.I., et al. 1987, ApJ 320, 356
Haschick A.D., Moran J.M., Rodríguez L.F., et al. 1980, ApJ 237, 26
Herbig G.H., Jones B.F., 1983, AJ 88, 1040
Hodapp K.-W., Ladd E.F., 1995, ApJ 453, 715
Lefloch B., Castets A., Cernicharo J., et al. 1998a, A&A 334, 269
Lefloch B., Castets A., Cernicharo J., et al. 1998b, ApJ , in press
Mauron N., Thouvenot E., 1991, IAU Circ., 5261
Molinari S., Liseau R., Lorenzetti D., 1993, A&AS 101, 59
Ossenkopf V., Henning T., 1994, A&A 291, 943
Pollack J.B., Hollenbach D., Beckwith S., et al. 1994, ApJ 421, 615
Rodríguez L.F., Cantó J. 1983, Rev. Mex. Astron. Astrofís. 8, 163
Rodríguez L.F., Anglada G., Curiel S., 1997, ApJ 480, L125
Sandell G., Aspin C., Duncan W.D., et al. 1990, A&A 232, 347
Schilke P., Walmsley C.M., Pineau des Fôrets G., et al. 1997, A&A 321, 293
Snell R., Bally J. 1986, ApJ 303, 683
Strom, S.E., Vrba, F.J., Strom, K.M. 1976, AJ 81, 314
Woody D.P., Scott S.L., Scoville N.Z., et al. 1989, ApJ 337, L41